an Article from

Journal of Robotics and Mechatronics

4F Toranomon Sangyo Bldg., 2-29, Toranomon 1-chome, Minatoku, Tokyo 105-0001, Japan
Tel. +813-3508-0051, Fax: +813-3592-0648, E-mail: robot@fujipress.jp
homepage URL: http://www.fujipress.jp/JRM/

Paper:

A Wearable Pointing Device Using EMG Signals

Hirotaka Ogino, Jun Arita, and Toshio Tsuji

Department of Artificial Complex Systems Engineering, Hiroshima University
1-4-1 Kagamiyama, Higashi-Hiroshima, Hiroshima 739-8527, Japan
E-mail: h_ogino@bsys.hiroshima-u.ac.jp
[Received October 17, 2004; accepted January 6, 2005]

We propose a wearable pointing device using EMG signals. By using neural networks, the system adapts to variations in EMG signals caused by individual differences of muscular features and minor shifts in electrode sites. Experimental results show that the system, which frees the operator from having to be in front of a computer, is effective as a pointing device for a wearable computer.

Keywords: pointing device, EMG signal, wearable computer, neural network

1. Introduction

With high-paced computer downsizing, so computers are becoming increasingly mobile, as shown by the appearance of wearable computers.

Wearable computer interfaces must occupy minimal space, be lightweight enough to wear, and require minimal operation space [1, 2], yet many pointing devices proposed for wearable computers are merely downsized conventional devices, physically limiting operator movement.

These problems are overcome by using physiological signals to develop a device enabling the operator to conduct pointing operations more intuitively while free from physical constraints. Attempts to use physiological signals for such interfacing include Rosenberg [3], who developed a two-dimensional pointing device for wearable computers, using EMG (electromyography) signals; and Barreto et al. [4], who developed a computer interface for the physically handicapped using EEG (electroencephalography) and EMG signals, enabling pointing in four directions and "clicks" using EEG frequency data and surface electromyogram signals.

We are developing a pointing device in which a neural network recognizes EMG signal patterns to move the pointer arbitrarily. Tsuji et al. [5] proposed an EMG-controlled pointing device with which the pointer is moved in an infinite number of arbitrary directions by expressing direction as a combination of a finite number of base directions. The direction of the pointer movement was estimated by calculating the posterior probability for each base direction using a log-linearized Gaussian mixture network (LLGMN), proposed by Tsuji et al. [6].

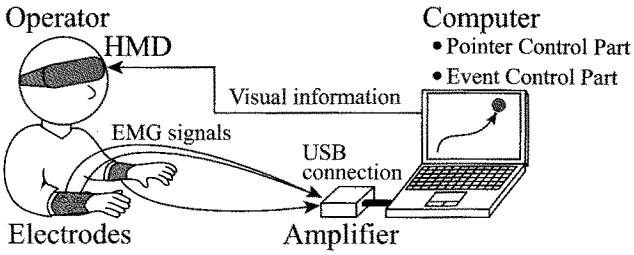

Fig. 1. Components of the prototype.

Considering the posterior probabilities to be vectors along the base directions, they were then summed to determine direction of the pointer movement [7]. Shortcomings included using a clinical-model EMG measurement device, making it unwieldy, and operating only in an exclusive application preventing its use for controlling pointers on commercial operating systems.

We propose an EMG signal-based wearable pointing device that overcomes these shortcomings, enabling the operator to control the pointer without physical constraints, and compact enough to be easily transportable. A neural network incorporated estimates "events" based on operator movement, enabling new event functions to be added and realize a multifunction pointing device. By training neural networks, the system adapts to individual variations in EMG signal patterns or minor shifts in electrode sites. The proposed system can be used for cursor control in Windows.

2. Wearable Pointing Device

2.1. System Configuration

In the prototype (**Fig.1**), electrodes for EMG measurement are attached to the operator via jockstraps wrapped around the arm and fastened (**Fig.2**).

A compact EMG measurement device developed for this study (**Fig.3**, **Table 1**) is transported easily because it is much smaller and lighter than conventional EMG measurement devices used in clinical situations. In the prototype, the operator wears a head mounted display (HMD) connected to the PC when conducting pointing operations.

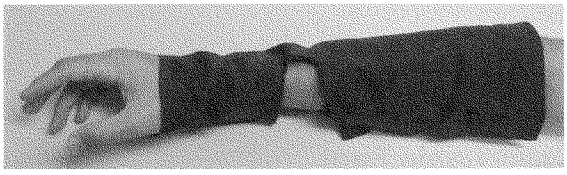

(a) Exterior

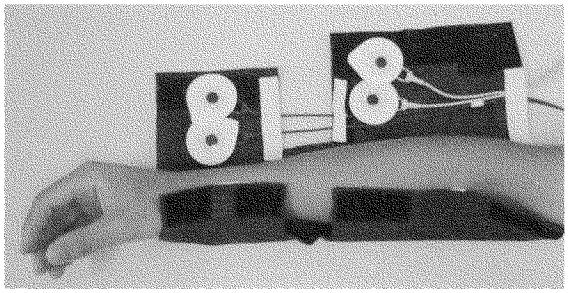

(b) Inner side of jockstrap

Fig. 2. A photo of electrodes.

Fig. 3. The measuring equipment of EMG signals.

Software on the PC consists of a pointer controller for measured EMG signals to move the pointer and an event controller that controls events such as "clicks", detailed in the sections that follow.

2.2. Pointer Controller

Figure 4 shows the pointer controller. First, The EMG signals for pointer control are measured and preprocessed. The neural network then estimates the direction of the pointer movement, and pointing is executed.

2.2.1. EMG Signal Processing

To process EMG signals, signals measured using L pairs of electrodes for pointer control are converted from analog to digital, and each channel is full-wave-rectified, then smoothed using a 2nd-order digital Butterworth filter (cutoff frequency: 1.0Hz). Time-series signals $EMG_l(n)$

Table 1. Specification of the measuring equipment.

Size	W150×H40×D100mm
Weight	0.33kg
Frequency response	10Hz-340Hz
Rate of amplification	About 2000
Measurement signal	EMG signal, 6CH
Power supply	USB
Current consumption	Under 50mA
CMRR	104dB
Resoluton	12bit (Succesive Approximation type)
Sampling frequency	1kHz

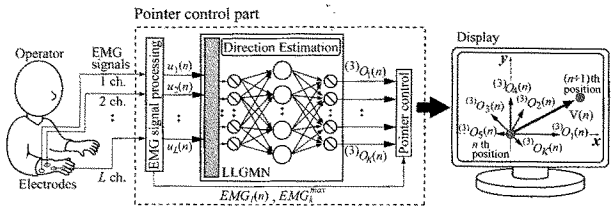

Fig. 4. Pointer control part.

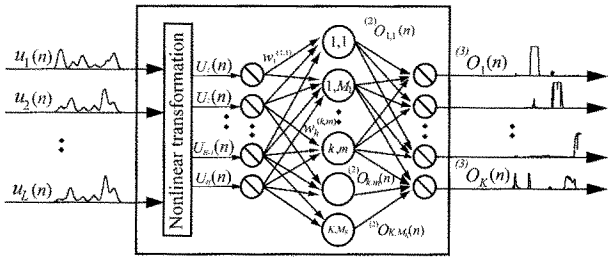

Fig. 5. Structure of the LLGMN.

$(l = 1, \cdots, L)$ thus obtained are used to calculate direction of the pointer movement and velocity. To estimate the direction, a feature pattern vector $\boldsymbol{u}(n) = [u_1(n), u_2(n), \cdots, u_L(n)]^{\mathrm{T}} \in \Re^L$, normalized so the sum of $EMG_l(n)$ for all channels equals unity, is used:

$$u_l(n) = \frac{EMG_l(n) - \overline{EMG_l^{st}}}{\sum_{l'=1}^{L} \left(EMG_{l'}(n) - \overline{EMG_{l'}^{st}} \right)} \quad \cdots\cdots \quad (1)$$

where $\overline{EMG_l^{st}}$ is the mean value of $EMG_l(n)$ while relaxing the muscle.

2.2.2. Estimation of Direction

LLGMN [6] (**Fig.5**) used as the neural network for estimating direction incorporates Gaussian mixture distribution and acquires statistical features of operator EMG signals by learning. Before the LLGMN is used for pointer control, it must first learn the relationship between operator EMG signal patterns and pointer directions [8]. Once trained, the LLGMN estimates from the statistical model the posterior probabilities of pointer movement in base

directions and outputs them from the output layer units corresponding to base directions [5].

To lessen the operator's psychological burden while waiting for learning to converge, a terminal attractor, proposed by Zak [9], was introduced in learning rules so a maximum could be set for conversion time.

2.2.3. Pointer Control

Pointer control calculates direction of the pointer movement and velocity from LLGMN output and estimates muscle contraction.

Output from the LLGMN's third layer (**Fig.4**) represents probability that the pointer will move in base direction k. Moving direction vector $\boldsymbol{e}(n) = (e_X(n), e_Y(n))^{\mathrm{T}}$ of the pointer generated by the nth EMG signal pattern is defined as follows:

$$e_X(n) = \frac{v_X(n)}{\sqrt{v_X^2(n)+v_Y^2(n)}} \quad \ldots\ldots\ldots (2)$$

$$e_Y(n) = \frac{v_Y(n)}{\sqrt{v_X^2(n)+v_Y^2(n)}} \quad \ldots\ldots\ldots (3)$$

$$v_X(n) = \sum_{k=1}^{K} {}^{(3)}O_k(n)\cos(2\pi(k-1)/K) \quad \ldots (4)$$

$$v_Y(n) = \sum_{k=1}^{K} {}^{(3)}O_k(n)\sin(2\pi(k-1)/K) \quad \ldots (5)$$

where $v_X(n)$ and $v_Y(n)$ are x and y components of vector elements corresponding to base directions.

Muscular contraction level $\alpha(n)$ is calculated as follows:

$$\alpha(n) = \frac{\sum_{l=1}^{L}\left(EMG_l(n) - \overline{EMG_l^{st}}\right)}{\sum_{k=1}^{K} EMG_k^{max}\,{}^{(3)}O_k(n)} \quad \ldots\ldots (6)$$

$$EMG_k^{max} = \sum_{l=1}^{L}\left(EMG_{kl}^{max}(n) - \overline{EMG_l^{st}}\right) \quad \ldots (7)$$

where $\overline{EMG_l^{st}}$ is the mean value of $EMG_l(n)$ while relaxing the muscle, ${}^{(3)}O_k(n)$ is the posterior probability of the base direction output by the neural network, and EMG_k^{max} is the channel sum of $EMG_{kl}^{max}(n)$ signals while keeping the maximum voluntary contraction for that base direction. The muscular contraction level is introduced to compensate somewhat for differences in maximal voluntary contraction in the different directions, and is used for computing the velocity of the pointer.

To ensure that the subjective feeling of pointer operation suits individual operators, pointer movement should satisfy common physical laws. The velocity of the pointer is calculated from muscular contraction level $\alpha(n)$ and the direction of the pointer movement $\boldsymbol{e}(n)$ using the following impedance model:

$$M_e\ddot{\boldsymbol{p}}(t) + B_e(r)\dot{\boldsymbol{p}}(t) = \boldsymbol{F}(t). \quad \ldots\ldots\ldots (8)$$

This equation of motion expresses the movement of a pointer with mass M_e lying in a space with variable viscosity $B_e(r)$ when it receives force $\boldsymbol{F}(t)$ by the operator. $\boldsymbol{p}(t)$ is the position vector of the pointer. Force $\boldsymbol{F}(t)$ exerted by the operator is calculated from $\alpha(n)$ and $\boldsymbol{e}(n)$ using a zero-order hold as follows:

$$\boldsymbol{F}(t) = \begin{cases} g\alpha(n\Delta t)\boldsymbol{e}(n\Delta t) & (\alpha(n\Delta t) \geq \alpha_0) \\ 0 & (\alpha(n\Delta t) < \alpha_0) \end{cases} \quad . \quad (9)$$

where $n\Delta t \leq t < (n+1)\Delta t$ holds, and Δt denotes sampling time, and g force gain. Threshold α_0 is used for judging whether a pointer operation takes place. Variable viscosity $B_e(r)$ in eq.(8) is defined as:

$$B_e(r) = \begin{cases} -\frac{B_u}{\pi}\tan^{-1}\{A(r-B)\} + \frac{B_u}{2} & (0 \leq r < r_0) \\ B_l & (r_0 \leq r) \end{cases} \quad . \quad (10)$$

$$B_l = -\frac{B_u}{\pi}\tan^{-1}\{A(r_0 - B)\} + \frac{B_u}{2} \quad \ldots (11)$$

where B_u is the maximum $B_e(r)$, A and B are positive constants, and r is pointer distance from its starting position. $B_e(r)$ is B_l when $r_0 < r$, beyond which viscosity remains constant until $\boldsymbol{F}(t) = 0$ irregardless of r. "Starting position" means screen coordinates of the pointer when $\boldsymbol{F}(t)$ exceeds 0, and the same starting position is kept until $\boldsymbol{F}(t) = 0$.

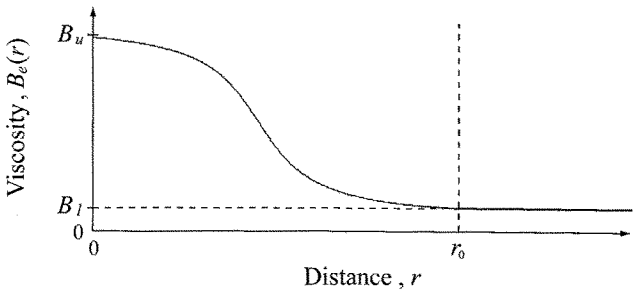

Fig. 6. Variable viscosity for pointer movement.

Figure 6 shows the viscosity curve when $A = 2$ and $B = 1$. When distance r is small and viscosity high, the operator controls the pointer in smaller increments to position the pointer accurately on a small target. For large distances when viscosity is low, the pointer is moved quickly with lower muscle contraction so the operator can move it quickly toward a distant target.

Using the impedance model to calculate pointer position and velocity, operational "feel" is expected to match operator muscle response. Variable viscosity in the model enables the operator to control the pointer more accurately, improving operability.

2.3. Event Controller

EMG signals measured from operator for event control are preprocessed (**Fig.7**), and then the neural network estimates the event and executes it.

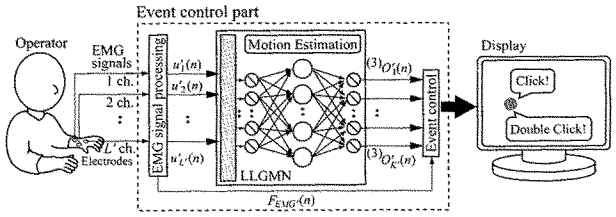

Fig. 7. Event control part.

2.3.1. EMG Signal Processing

EMG signals measured using L^I pairs of electrodes, attached to a different area, e.g., the left forearm, are processed similar to that in Section 2.2.1 to obtain $EMG^I_{l^I}(n)(l^I = 1, \cdots, L^I)$. A feature pattern vector $\boldsymbol{u}^I(n) = [u^I_1(n), u^I_2(n), \cdots, u^I_{L^I}(n)]^{\mathrm{T}} \in \Re^{L^I}$, normalized so the sum of $EMG^I_{l^I}(n)$ for all channels equals unity, is input to the LLGMN. As information on muscle force associated with input $\boldsymbol{u}^I(n)$ to the neural network in **Fig.7**, $F_{EMG^I}(n)$ is calculated as follows:

$$F_{EMG^I}(n) = \frac{1}{L^I} \sum_{l^I=1}^{L^I} \frac{EMG^I_{l^I}(n) - \overline{EMG^I_{l^I}}^{st}}{EMG^{I\,max}_{l^I} - \overline{EMG^I_{l^I}}^{st}} \quad \cdots \quad (12)$$

where $EMG^{I\,max}_{l^I}$ is $EMG^I_{l^I}(n)$ during maximal voluntary contraction.

2.3.2. Estimation of Event

LLGMN different from that used to estimate direction of the pointer movement is used to estimate events. Before the LLGMN is used for event control, it must learn the relationship between operator EMG signal patterns and operator arm movement, each corresponding to some event. Once trained, the LLGMN estimates from the statistical model the posterior probabilities of movements, and outputs them from output layer units corresponding to events.

In forward calculation, nonlinear transformation is done on input vector $\boldsymbol{u}^I(n)$, as in section 2.2.2, to generate new input vector $\boldsymbol{U}^I(n)$, then posterior probabilities ${}^{(3)}O^I_{k^I}(n)(k^I = 1, \cdots, K^I)$ are output from units of the third layer, which consists of K^I events.

For training, D^I data sets of EMG signals for movement, e.g., wrist flexion or extension, corresponding to an event are extracted for each event to form a sample data set of $N^I(= K^I \times D^I)$ data. The training signal given to units in the third layer generated by n-th input vector $\boldsymbol{u}^I(n)$ is defined as $\boldsymbol{T}^I(n) = [T^I_1(n), \cdots, T^I_{k^I}(n), \cdots, T^I_{K^I}(n)]^{\mathrm{T}}$. $T^I_{k^I}(n)$ is 1 when the event is k^I, and 0 otherwise. Just as for the LLGMN for pointer control in section 2.2.2, a terminal attractor [9] was introduced into learning rules so learning takes place in a limited time.

2.3.3. Event Control

In event control, data obtained as described in section 2.3.1 is used for event recognition and the event intended by the operator is executed.

EMG data is used to determine whether an event should take place, and estimated muscle force $F_{EMG^I}(n)$, obtained in section 2.3.1, is compared to event generation threshold M_d. Events are thus recognized only when the threshold is exceeded and it is determined that an event has been generated.

To improve the accuracy of determining the event intended by the operator, LLGMN output entropy is used for recognition as an indicator of ambiguity of information to prevent ambiguous recognition [10]. Entropy is calculated from output ${}^{(3)}O^I_{k^I}(n)$ from the LLGMN as follows:

$$H(n) = -\sum_{k^I=1}^{K^I} {}^{(3)}O^I_{k^I}(n) \log {}^{(3)}O^I_{k^I}(n) \quad \cdots \quad (13)$$

Whether to suspend recognition is based on a comparison of $H(n)$ with threshold H_d. If $H(n) < H_d$, the event corresponding to the unit with the largest output ${}^{(3)}O^I_{k^I}(n)$ is selected and executed. If $H(n) > H_d$, recognition is ambiguous and suspended.

The operator selects event settings, including event types and correspondence between events and body movement, adding functions such as "double click" and "scrolling" in addition to left and right "clicks", or eliminating the "right click" and retaining only the "left click" and "double click". The result is a multifunction pointing device in which events are easily added or deleted to suit individual operators.

The proposed pointing device features the following:

- No physical constraints on the operator. The device uses EMG signals from electrodes as an interface, unlike a mouse or keyboard, which requires operating space.
- Stable, robust operation. Individual differences among operators, shifts in electrode sites, or variations in skin resistance caused by perspiration, etc., are assimilated due to adaptive learning of neural networks.
- By applying a physical model (i.e., motion of a body with inertial mass in a variable viscosity field) to the pointer's movement, it is possible to realize an operability that suits the operator's muscle sense.
- Readily changed pointer functions. A neural network estimating events such as "clicks" enables the operator to easily change functional settings.
- Compact EMG measurement. The pointing device is suitable for use with a wearable computer.

3. Experiment

An experiment was done to test the feasibility of the prototype. Subjects were 3 healthy male students aged 22, 23, and 23. Subjects were given time to practice until they were proficient in system use.

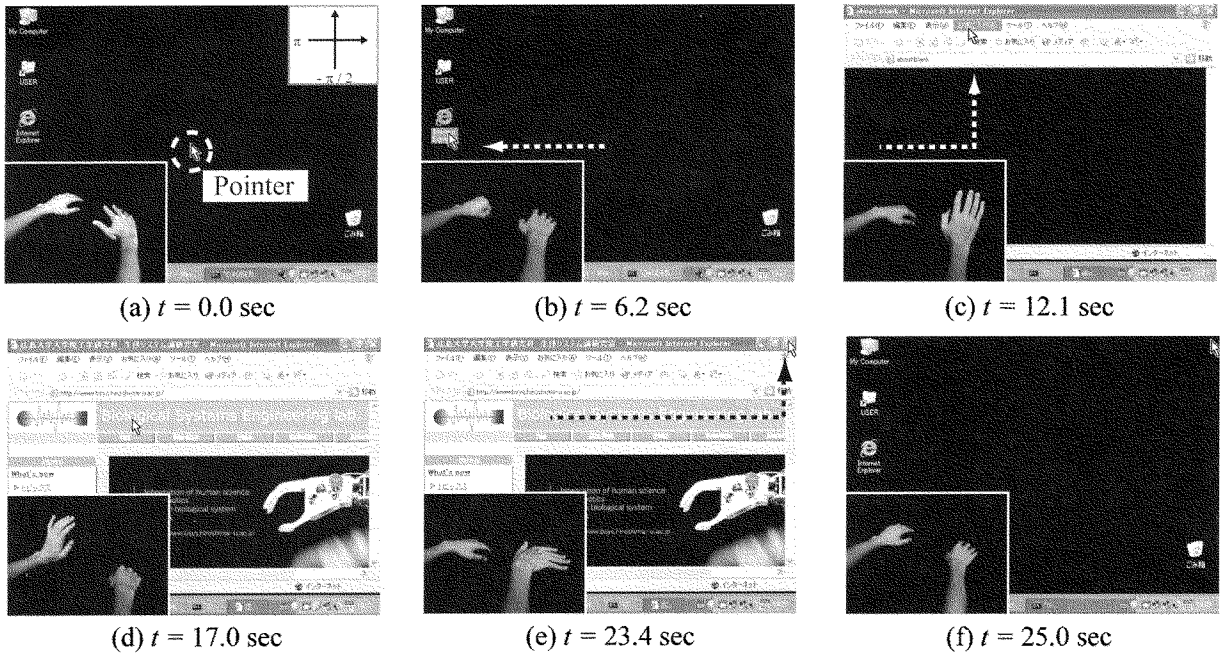

(a) $t = 0.0$ sec (b) $t = 6.2$ sec (c) $t = 12.1$ sec

(d) $t = 17.0$ sec (e) $t = 23.4$ sec (f) $t = 25.0$ sec

Fig. 8. A series of photos while manipulating the proposed system.

Bipolar differential electrodes were used to measure EMG siganals. Six pairs were used – 4 on the right forearm ($L = 4$; M. extensor carpi radialis, M. flexor carpi ulnaris, M. extensor carpi ulnaris, and M. extensor pollicis longus) for pointer control, and 2 on the left forearm ($L' = 2$; M. extensor carpi radialis and M. flexor carpi ulnaris) for event control. Note that a certain amount of shifting is allowed for the electrode positions because the neural networks introduced in the system are capable of adaptation. This is particularly useful in a wearable pointing device, where it would be impractical to require electrodes to be attached to specific muscles each time it is used.

In the experiment, pointer movement was associated with right wrist bending, and the neural network was trained accordingly. Events such as "clicks" were controlled by left hand movement.

The data sampling frequency was 1000Hz, and the number of components and learning sample data, which are LLGMN parameters, were set at $M_k = M_{k'} = 1$ and $D' = 20$. The 4 directions ($K = 4$), $f = 0, \pi/2, 3\pi/2, 2\pi$rad, were set as base directions for training the LLGMN for pointer control. Terminal attractor parameters, common to both LLGMNs, were set at learning time $t_f = 1$, learning rate $\beta = 0.5$, and sampling time $\Delta t = 0.001$.

3.1. Example of Operation

The proposed system was used to operate a software application. Subject was asked to "double click" to start a Web browser, go to a specified web page, then exit the browser. When providing training data to the LLGMN for pointer control, the four directions, $f = 0, \pi/2, 3\pi/2, 2\pi$rad, were used for measuring directions. The number of events was set at $K' = 3$, and dorsiflexion of the wrist, palmar flexion of the wrist, and grip were associated with "left click", "right click", and "double click". Other parameters were set as follows: $\alpha_0 = 0.5$, $M_d = 0.25$, $H_d = 0.15$, $g = 20$N, $M_e = 5.0$Ns^2/pixel, $B_u = 5.0$Ns/pixel, $A = 3.5$, $B = 1.0$, and $r_0 = 0$ pixel.

Figures 8 and **9** show examples of experiment results for subject A. **Fig.8** shows photos of the subject's hands and corresponding operations on the monitor display. **Fig.9** shows processing data during operations. **Fig.9(a)** gives results of the right arm, consisting of, from top to bottom, EMG signals, muscular contraction level $\alpha(n)$, and the estimated pointer direction. Shaded areas are intervals for which it was determined from muscular contraction level that no operation took place. **Fig.9(b)** gives results of the left arm, consisting of, from top to bottom, EMG signals, muscular contraction level, entropy, and discrimination results (i.e., events). Shaded areas represent intervals when an operational event took place. Gripping at (A) in **Fig.9(b)**, corresponding to a "double click", starts the software application (**Fig.8(b)-(c)**). Dorsiflexion, i.e., bending back, of the wrist, representing a "left click", at time (B) exits the application (**Fig.8(e)-(f)**). This example shows that the system starts up a Windows application and conducts intended operations.

3.2. Validity of Variable Viscosity Model

The next experiment was conducted to evaluate the validity of the impedance model introduced for the pointer controller (**Fig.10**). A subject was asked to move the pointer from the "start position" to the "target" and to "left click" on the target as quickly as possible. The experiment measured time from the moment the subject begins moving the pointer until "left click" is executed. Four base di-

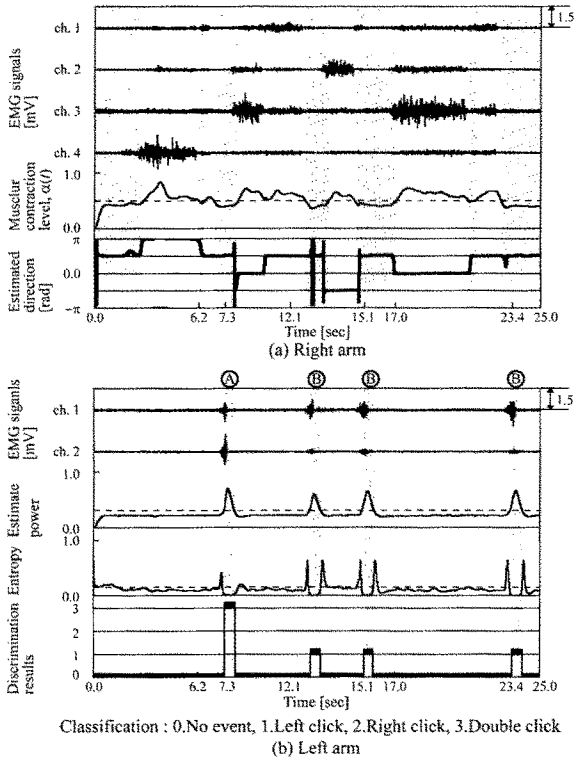

Fig. 9. An example of the pointer control.

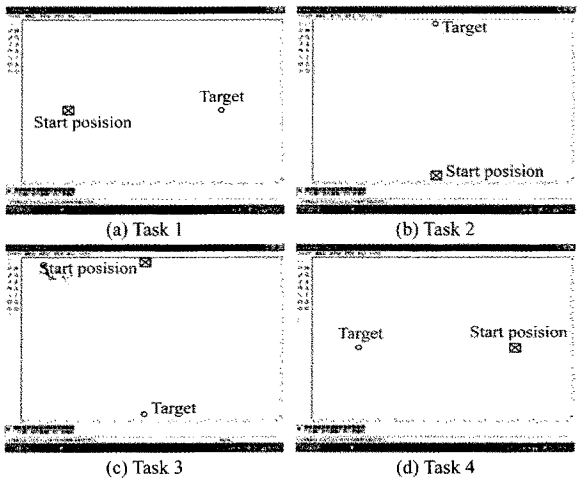

Fig. 10. Experimental conditions for performance analysis.

Table 2. Results of comparative experiments.

(a) Proposed method using variable viscosity [sec]

	Task 1	Task 2	Task 3	Task 4	Mean
subject A	4.88 ± 0.29*	4.05 ± 1.38	4.52 ± 0.64*	4.53 ± 1.07	4.49 ± 0.34**
subject B	5.07 ± 2.03	3.40 ± 1.42	3.03 ± 0.49**	4.63 ± 1.99**	4.03 ± 0.97**
subject C	4.42 ± 0.61**	5.40 ± 1.51*	4.02 ± 0.63**	5.41 ± 1.20	5.19 ± 0.76**

*···5%, **···1%

(b) Authors' previous method using constant viscosity [sec]

	Task 1	Task 2	Task 3	Task 4	Mean
subject A	5.43 ± 2.47	7.11 ± 3.93	5.59 ± 1.79	5.02 ± 1.92	5.89 ± 0.91
subject B	5.72 ± 2.21	5.04 ± 3.36	8.43 ± 4.36	8.53 ± 1.81	6.93 ± 1.81
subject C	6.87 ± 2.71	7.31 ± 2.84	6.79 ± 3.21	6.73 ± 1.83	7.48 ± 0.29

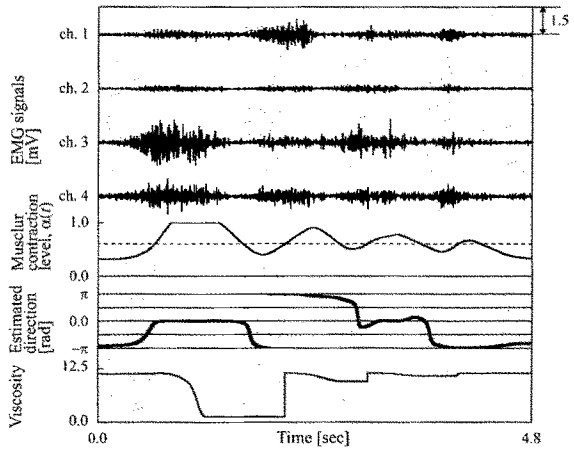

(a) The variable viscosity

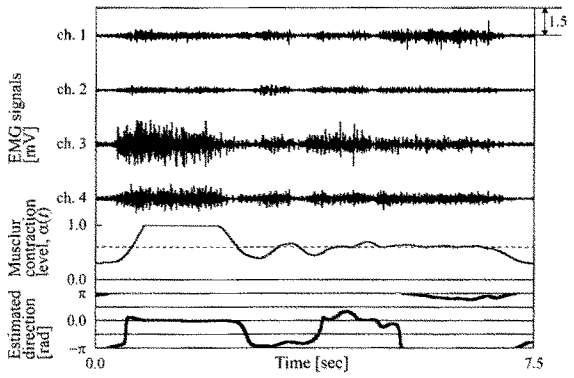

(b) The constant viscosity ($B_e(r) = 5.0$Ns/pixel)

Fig. 11. An example of the experimental results.

rections were used for measuring directions when providing training data to the LLGMN for pointer control. Parameters were set as follows: $\alpha_0 = 0.5$, $M_d = 0.25$, $H_d = 0.15$, $g = 20$N, $M_e = 5.0$Ns^2/pixel, $B_u = 12.5$Ns/pixel, $A = 3.5$, $B = 1.0$, and $r_0 = 90$ pixel. Setting the distance between the "start position" and "target" at 565 pixels, and using the four base directions, up, down, right, and left, as the direction of the pointer movement, measurement was done with and without variable viscosity. When not in use, viscosity was kept constant at an appropriate value for moving the pointer. A single session consisted of four tasks of moving the pointer in each of the four directions. Seven sessions each were done, with and without variable viscosity. For each set of seven sessions, maximum and minimum results were discarded, and the mean and standard deviation were obtained from the remaining five sessions.

Table 2 presents experimental results, and **Fig.11** shows examples of signal processing results. **Table 2(a)** is when variable viscosity was introduced, and **Table 2(b)** when a constant viscosity was used. Asterisks * and ** indicate results for which there were significant differences at risk factors of 5% and 1%, based on a one-tailed test in which the result with variable viscosity was used as

the reference. **Table 2** shows that, for all four directions, the mean arrival time and its standard deviation are both smaller when variable viscosity is used, showing that it results in stabler operation. **Fig.11(a)** gives results when variable viscosity was used, showing from top to bottom EMG signals, muscular contraction level $\alpha(n)$, direction of the pointer movement, and viscosity. Shaded areas are intervals for which it was determined from the muscular contraction level that no operation took place. **Fig.11(b)** gives results when variable viscosity was not used, showing from top to bottom EMG signals, muscular contraction level $\alpha(n)$, and direction of the pointer movement. **Fig.11(a)** shows varying viscosity $B_e(r)$. Less fluctuation occurs in the direction of the pointer movement direction compared to **Fig.11(b)**, showing that introducting variable viscosity improves operability.

4. Conclusions

To develop an EMG signal-based pointing device for wearable computers, we designed a prototype operated in a Windows environment as a pointing device for wearable computers, readily transportable because the EMG measurement device is compact. A neural network estimates "events" based on operator movement and lets new event functions be added easily, realizing a multifunction pointing device.

Experiments verified that EMG signals acquired from a compact EMG measurement device are used to conduct pointing operations accurately and execute events such as "clicks" in a Windows environment. An experiment comparing impedance models incorporating variable and non-variable viscosity showed that variable viscosity improves operability.

In future work, we will improve the neural network for estimating pointer direction by improving its estimation accuracy, and also improve the hardware components, including the development of electrodes that are easily "worn" and removed, in an effort to construct a system that achieves higher levels of practicality.

References:

[1] S. Mann, "Wearable Computing: A First Step Toward Personal Imaging," IEEE Computer, Vol.30, No.2, pp. 25-32, 1997.

[2] T. Inoue, N. Kamijo, and K. Tamagawa, "Present State and Future Prospect of Wearable Computers," Journal of the Robotics Society of Japan, Vol.20, No.8, pp. 791-795, 2002 (in Japanese).

[3] R. Rosenberg, "The Biofeedback Pointer: EMG Control of a Two Dimensional Pointer," Proceedings of the 2nd International Symposium on Wearable Computers, pp. 162-163, 1998.

[4] A. B. Barreto, S. D. Scargle, and M. Adjouadi, "A Practical EMG-based Human-computer Interface for Users with Motor Disabilities," Journal of Rehabilitation Research and Development, Vol.37, No.1, pp. 55-63, 2000.

[5] T. Tsuji, O. Fukuda, M. Murakami, and M. Kaneko, "An EMG Controlled Pointing Device Using a Neural Network," Trans. of the Society of Instrument and Control Engineers, Vol.37, No.5, pp. 425-431, 2004 (in Japanese).

[6] T. Tsuji, H. Ichinobu, and M. Kaneko, "A Proposal of the Feedforward Neural Network Based on the Gaussian Mixture Model and the Log-Linear Model," Trans. Institute of Electronics, Information and Communication Engineers, D-II, Vol.J77, No.10, pp. 2093-2100, 1994 (in Japanese).

[7] O. Fukuda, J. Arita, and T. Tsuji, "An EMG-Controlled Omnidirectional Pointing Device," Trans. Institute of Electronics, Information and Communication Engineers, D-II, Vol.J87, No.10, pp. 1996-2003, 2004 (in Japanese).

[8] O. Fukuda, T. Tsuji, and M. Kaneko, "An EMG Controlled Robotic Manipulator Using Neural Networks," Proceedings of IEEE International Workshop on Robot and Human Communication, pp. 442-447, 1997.

[9] M. Zak, "Terminal Attractors for Addressable Memory in Neural Network," Physics Letters A, Vol.133, pp. 18-22, 1998.

[10] O. Fukuda, T. Tsuji, and M. Kaneko, "A Human Supporting Manipulator Based on Manual Control Using EMG Signals," Journal of the Robotics Society of Japan, Vol.18, No.3, pp. 387-394, 2000 (in Japanese).

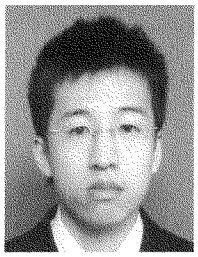

Name:
Hirotaka Ogino

Affiliation:
Department of Artificial Complex Systems Engineering, Hiroshima University

Address:
1-4-1 Kagamiyama, Higashi-Hiroshima, Hiroshima 739-8527, Japan

Brief Biographical History:
2004- Graduate School of Engineering, Hiroshima University

Name:
Jun Arita

Affiliation:
Department of Artificial Complex Systems Engineering, Hiroshima University

Address:
1-4-1 Kagamiyama, Higashi-Hiroshima, Hiroshima 739-8527, Japan

Brief Biographical History:
2003- Graduate School of Engineering, Hiroshima University

Main Works:
• "An EMG-Controlled Omnidirectional Pointing Device," IEICE Trans. Inf. & Syst., Pt.2 (Japanese Edition), D-II, Vol.J87, No.10, pp. 1996-2003, 2004.

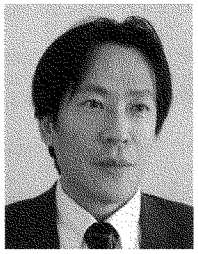

Name:
Toshio Tsuji

Affiliation:
Department of Artificial Complex Systems Engineering, Hiroshima University

Address:
1-4-1 Kagamiyama, Higashi-Hiroshima, Hiroshima 739-8527, Japan

Brief Biographical History:
1985- Research Associate at Hiroshima University
1995- Associate Professor at Hiroshima University
2002- Professor at Hiroshima University

Main Works:
- "A Human-Assisting Manipulator Teleoperated by EMG Signals and Arm Motions," IEEE Transactions on Robotics and Automation, Vol.19, No.2, pp. 210-222, April 2003.
- "A Recurrent Log-linearized Gaussian Mixture Network," IEEE Transactions on Neural Networks, Vol.14, No.2, pp. 304-316, March 2003.

Membership in Learned Societies:
- IEEE
- The Japan Society of Mechanical Engineers
- The Robotics Society of Japan
- The Japanese Society of Instrumentation and Control Engineers